

Strictly invariant sets for 2-D tent maps: 2-D strange attractors

A. Marqués-Lobeiras ¹, A. Pumariño ¹,
J. Á. Rodríguez ¹ and E. Vigil ¹

Abstract We study the existence of maximal strictly invariant compact sets for a certain two-parameter family of Expanding Baker Maps (EBMs), called 2-D tent maps. If, in addition, these sets are minimal, then they will be attractors. Since EBMs are expansive, these attractors will be 2-D strange attractors provided that they have non-empty interior. The results and proposals stated in this work will be essential to prove the existence of 2-D strange attractors for the quadratic family $T_{a,b}(x, y) = (a + y^2, x + by)$. Such family appears as a family of limit return maps in the unfolding of certain generalized homoclinic tangencies of 3-D diffeomorphisms.

1 Introduction

The most significant elements of the phase portrait of dissipative dynamical systems are their *attractors*. These sets compete against each other to attract towards themselves the orbits of the system making their internal dynamics observable.

Definition 1 A n a ttractor for a map $f: M \rightarrow M$ on a manifold M is a transitive f -invariant compact set \mathcal{A} whose stable set

$$W^s(\mathcal{A}) = \{z \in M : d(f^n(z), \mathcal{A}) \rightarrow 0 \text{ as } n \rightarrow \infty\}$$

has non-empty interior.

Since every attractor \mathcal{A} is transitive, then \mathcal{A} is *minimal*, i.e. it contains no proper invariant compact set with non-empty interior. Therefore, \mathcal{A} is strictly f -invariant, i.e. $f(\mathcal{A}) = \mathcal{A}$, whenever f is continuous. The simplest examples of

✉ E. Vigil
E-mail: vigilkike@gmail.com

¹ Dep. de Matemáticas. c\ Federico García Lorca 18, 33007, Univ. de Oviedo. Spain

attractors are periodic orbits, closed curves, and tori. In the past century, other attractors with a fractal structure and a very complicated internal dynamics were found. Arbitrarily small deviations on the initial conditions grow ever larger along such attractors, making it impossible to predict the dynamics—thus arose the idea of chaotic dynamics and the concept of *strange attractor*.

Definition 2 An attractor \mathcal{A} for a map $f: M \rightarrow M$ is said to be *strange* if it contains a dense orbit $\{f^n(z_1) : n \geq 0\}$ displaying exponential growth of the derivative, i.e. there exist a unit vector v and a constant $c > 0$ such that, for all $n \geq 0$,

$$\|Df^n(z_1)(v)\| \geq e^{cn}.$$

The supremum of such c is called a *Lyapunov exponent*.

The observability of an attractor, or actually of any dynamics, requires some kind of robustness to survive small perturbations of the system. Namely, maps sufficiently close in some topology (the C^1 -topology, for example) must have equivalent dynamics.

Definition 3 An attractor \mathcal{A} for a map $f: M \rightarrow M$ is said to be *structurally stable* if every sufficiently C^1 -close map $g: M \rightarrow M$ also has an attractor $\mathcal{A}(g)$ that is *conjugate* to \mathcal{A} , i.e. there exists a homeomorphism $h: \mathcal{A} \rightarrow \mathcal{A}(g)$ such that $g|_{\mathcal{A}(g)} \circ h = h \circ f|_{\mathcal{A}}$. The homeomorphism h is called a *conjugation*.

It was proved in [12] that structural stability is equivalent to uniform hyperbolicity in the set of C^1 -diffeomorphisms on M . Previously, some hyperbolic strange attractors had been ingeniously devised (e.g. Smale's solenoid [27]). However, examples as simple as the 3-D quadratic vector field of Lorenz [11] or the 2-D quadratic diffeomorphism of Hénon [10] displayed attractors with a complicated structure and an unpredictable dynamics which are not structurally stable, and therefore, are not uniformly hyperbolic. At that point there arose a natural question: Do there really exist for the set of C^1 -diffeomorphisms on M non-uniformly hyperbolic strange attractors with some kind of persistence making them observable?

The first positive answer was provided by Benedicks and Carleson [4] for the Hénon family

$$H_{a,b}(x, y) = (1 - ax^2 + y, bx). \quad (1)$$

The authors proved that for arbitrarily small $b > 0$ and for values of a sufficiently close to 2, the Hénon family has strange attractors *persistent* in the measure sense.

Definition 4 Let $f_\mu: M \rightarrow M$ be a continuous family of maps. Assume that f_μ has a strange attractor \mathcal{A} for some $\mu = \mu_0$. We say that \mathcal{A} is *persistent (in the measure sense)*, or that it *occurs with positive probability*, if for every $\delta > 0$ there exists $E_\delta \subseteq B(\mu_0, \delta)$ with positive Lebesgue measure such that f_μ has a strange attractor for all $\mu \in E_\delta$. If $E_\delta = B(\mu_0, \delta)$ for some $\delta > 0$, then \mathcal{A} is said to be *fully persistent*.

The proof of the existence of strange attractors in [4] is very hard. One has to start by observing that the dynamics of (1) for $b = 0$ is the dynamics of the quadratic family

$$f_a(x) = 1 - ax^2 \quad (2)$$

and then, the dynamics of this limit family is transferred to one of the branches of the unstable manifold of the saddle fixed point of (1) arising for $b > 0$. Actually, the same authors had already proved in [3] that family (2) has persistent strange attractors for a set of parameters with positive Lebesgue measure near $a = 2$.

In a simpler scenario, fully persistent strange attractors had been found for the family $\{\lambda_\mu\}_{\mu \in (1,2]}$ of tent maps given by

$$\lambda_\mu(x) = \begin{cases} \mu x & \text{if } 0 \leq x \leq 1, \\ \mu(2-x) & \text{if } 1 \leq x \leq 2. \end{cases} \quad (3)$$

Clearly, the interval $I_\mu = [\mu(2-\mu), \mu]$ is strictly λ_μ -invariant for every $\mu \in (1, 2]$. In fact, I_μ is a strange attractor for every $\mu \in (\sqrt{2}, 2]$ and is limited by the first iterates of the critical point. Iterating the critical set will also be our strategy for looking for strange attractors in the 2-D setting of this paper.

Strange attractors with several pieces can also be obtained for $\mu \in (1, \sqrt{2}]$ by means of renormalization techniques (for related details, see [5], [8], or [9]). In many cases, the dynamics of family (3) is conjugate to that of family (2). It is well-known that this is the case when, for instance, we choose $\mu = a = 2$.

Persistent strange attractors play an important role in non-uniformly hyperbolic dynamics. They appear generically close to homoclinic points. As it was proved in [13], a generic one-parameter family of diffeomorphisms f_μ defined on a surface which has a homoclinic tangency for some $\mu = \mu_0$ displays, for values of μ sufficiently close to μ_0 , persistent strange attractors. See [16, 17] for the coexistence of persistent strange attractors in a neighbourhood of a homoclinic orbit of a family of 3-D vector fields.

The idea of taking advantage of the dynamics of families of limit return maps was used in [13]. In order to be more precise, we must remark that the main result in [13], as well as many others (see [7], [14], [15], and [30]), is strongly based on the existence of families of limit return maps associated to the unfolding of homoclinic tangencies. Under an appropriate change of coordinates, these return maps are defined in a neighborhood of the homoclinic point and they are very similar to the ones defined in (1). This is the reason why they were called Hénon-like maps.

All the above-mentioned attractors are one-dimensional. The existence of strange attractors of an ever greater dimension is the key to establishing a certain hierarchy on the understanding of the dynamical complexity arising in nature. In order to get abundance of higher-dimensional strange attractors, a saddle fixed point with an unstable manifold of dimension greater than or equal to 2 becomes necessary. We may consider a generic two-parameter family $f_{a,b}: M \rightarrow M$ of 3-D diffeomorphisms unfolding a *generalized homoclinic tangency*, as it was originally defined in [28, p. 272]. Then, the unstable manifold

of the periodic orbit involved in the homoclinic tangency is two-dimensional and the limit family is conjugate to the family of two-dimensional quadratic maps given by

$$T_{a,b}(x, y) = (a + y^2, x + by). \quad (4)$$

With a view to showing the existence of 2-D strange attractors when the 3-D homoclinic tangency is unfolded, the first step should be to demonstrate, as was done in the 1-D setting, the existence of strange attractors for the limit family (4). Only then will it make sense to lift the dynamics to the closure of the unstable manifold, which is the candidate to be the two-dimensional strange attractor arising in the unfolding of the tangency.

The dynamical behaviour of family (4) is rather complicated as was numerically shown in [25] and, in particular, the attractors exhibited by $T_{a,b}$ for a large set of parameters seem to be 2-D strange attractors. Moreover, in [24], a curve of parameters $G = G(s) = \{(a(s), b(s))\}$ was constructed in such a way that $T_{a(s),b(s)}$ has an invariant region in \mathbb{R}^2 that is homeomorphic to a triangle for all $s \leq 2$. In particular, for $s = 2$, $a(2) = -4$ and $b(2) = -2$, and the map $T_{-4,-2}$ is conjugate to the non-invertible piecewise affine map

$$\Lambda(x, y) = \begin{cases} (x + y, x - y) & \text{if } (x, y) \in \mathcal{T}_0, \\ (2 - x + y, 2 - x - y) & \text{if } (x, y) \in \mathcal{T}_1, \end{cases} \quad (5)$$

defined on the triangle $\mathcal{T} = \mathcal{T}_0 \cup \mathcal{T}_1$, where $\mathcal{T}_0 = \{0 \leq x \leq 1, 0 \leq y \leq x\}$ and $\mathcal{T}_1 = \{1 \leq x \leq 2, 0 \leq y \leq 2 - x\}$.

As was pointed out in [24], the map Λ enjoys the same nice properties as the 1-D tent map λ_2 in (3). In particular, the consecutive pre-images $\{\Lambda^{-n}(\mathcal{C})\}_{n \in \mathbb{N}}$ of the critical line $\mathcal{C} = \{(x, y) \in \mathcal{T} : x = 1\}$ define a sequence of partitions (whose diameter tends to zero as n goes to infinity) of \mathcal{T} leading the authors to conjugate Λ (and therefore $T_{-4,-2}$) to a one-sided shift on two symbols. Furthermore, for every initial point $(x_0, y_0) \in \mathcal{T}$ whose orbit never visits the critical line, the Lyapunov exponent of Λ along the orbit of (x_0, y_0) is positive (in fact, it is equal to $\frac{1}{2} \ln 2$) in all non-zero direction and the same holds for the limit return map $T_{-4,-2}$. Finally, an absolutely continuous ergodic invariant measure for Λ can be constructed, and therefore the same holds for $T_{-4,-2}$. These basically were the main reasons why the authors in [24] called Λ the 2-D tent map.

As a first approach to studying the dynamics of $T_{a(s),b(s)}$ for s close to 2, the family $\{\Lambda_t\}_{t \in (0,1]}$ of piecewise affine self-maps of \mathcal{T} given by

$$\Lambda_t(x, y) = t \cdot \Lambda(x, y) = \begin{cases} (t(x + y), t(x - y)) & \text{if } (x, y) \in \mathcal{T}_0, \\ (t(2 - x + y), t(2 - x - y)) & \text{if } (x, y) \in \mathcal{T}_1, \end{cases} \quad (6)$$

was introduced in [19]. The study of the dynamics exhibited by family (6) is mainly justified when one compares its attractors (numerically obtained in [18]) with the attractors (numerically obtained in [25]) for the family $T_{a,b}$ with $(a, b) \in G$. For different values of the parameters, both families of maps display convex strange attractors, connected (but not simply-connected) strange

attractors, and non-connected strange attractors (formed by numerous connected pieces).

A first analytical proof of the existence of a convex strange attractor for A_t was given in [20] for $t_0 < t < 1$, where $t_0 = 2^{-\frac{1}{2}}(1+\sqrt{2})^{\frac{1}{4}}$, and, as it was seen in [24] for $t = 1$, it was also proved that the attractor supports a unique ergodic invariant probability measure for all $t \in (t_0, 1]$. The existence of persistent strange attractors with several pieces for $2^{-\frac{1}{2}} < t < 2^{-\frac{2}{5}}$ is proved from [21], [22] and [23]. The proof is a consequence of a renormalization procedure that allows us to understand how connected invariant compact sets (formed by a unique piece) may split giving rise to others formed by an increasing number n of pieces. Then, from Theorem 1.2 in [23] it follows that these new disconnected invariant compact sets contain strange attractors formed by n pieces.

Just as the dynamics of family (3) approximates the dynamics of family (2), the dynamics of family (4) for $(a, b) \in G$ was approximated by the dynamics of family (6) throughout [18, 19, 20, 21, 22, 23]. However, the whole family (4) is a two-parameter one, which makes it necessary to choose a two-parameter family of piecewise affine maps that approximate the dynamics of family (4) for values of the parameters outside the curve G . For this reason, we will consider in this paper the family $\{\Gamma_{a,\theta} : (a, \theta) \in (1, \infty) \times (0, \pi)\}$ given in the complex variable $z = x + iy$ by

$$\Gamma_{a,\theta}(x + iy) = \begin{cases} a \cdot e^{i\theta}(x + iy) & \text{if } x \leq 1, \\ a \cdot e^{i\theta}(2 - x + iy) & \text{if } x \geq 1. \end{cases} \quad (7)$$

Note that $\Gamma_{a,\theta}$ is the composition of the fold

$$\mathcal{F}(x + iy) = 1 - |1 - x| + iy$$

and the expanding linear map $A_{a,\theta}(z) = ae^{i\theta}z$.

Definition 5 Let $\mathcal{K} \subseteq \mathbb{R}^2$ be a set with non-empty interior. Let \mathcal{L} be a line in \mathbb{R}^2 intersecting the interior of \mathcal{K} . The line \mathcal{L} splits \mathcal{K} into two sets \mathcal{K}_0 and \mathcal{K}_1 , i.e. $\mathcal{K}_0 \cup \mathcal{K}_1 = \mathcal{K}$ and $\mathcal{K}_0 \cap \mathcal{K}_1 = \mathcal{L} \cap \mathcal{K}$. Let $P \in \mathcal{K}_0$. The *fold* with respect to \mathcal{L} onto P for \mathcal{K} is the map $\mathcal{F}_{\mathcal{L},P} : \mathcal{K} \rightarrow \mathbb{R}^2$ given by

$$\mathcal{F}_{\mathcal{L},P}(Q) = \begin{cases} Q & \text{if } Q \in \mathcal{K}_0, \\ \tilde{Q} & \text{if } Q \in \mathcal{K}_1, \end{cases}$$

where \tilde{Q} denotes the symmetric point of Q with respect to \mathcal{L} . If $\mathcal{F}_{\mathcal{L},P}(\mathcal{K}) = \mathcal{K}_0$, we say that $\mathcal{F}_{\mathcal{L},P}$ is a *good fold* for \mathcal{K} .

For the folds considered in this work, the line \mathcal{L} will be $\mathcal{C} = \{x = 1\}$ and the point P will be the origin \mathcal{O} .

Definition 6 Let $\mathcal{K} \subset \mathbb{R}^2$ be a set with non-empty interior such that $\mathcal{O} \in \mathcal{K}$. Let $\mathcal{F}_{\mathcal{L},\mathcal{O}}$ be a good fold for \mathcal{K} . An *Expanding Baker Map* (EBM) is the composition of $\mathcal{F}_{\mathcal{L},\mathcal{O}}$ with an expanding linear map $A : \mathbb{R}^2 \rightarrow \mathbb{R}^2$ such that $A(\mathcal{K}_0) \subseteq \mathcal{K}$. For short, we will denote them by $EBM(\mathcal{L}, \mathcal{O}, A)$.

For a definition of EBM in more general contexts, see [21].

Remark 1 By performing a suitable affine change of coordinates, the map A_t is transformed into $\Gamma_{a,\theta}$ with $a = \sqrt{2}t$ and $\theta = 3\pi/4$.

Therefore, an interesting program of work arises immediately: trying to prove, for the general family $\Gamma_{a,\theta}$, the results stated for the family A_t in [20, 21, 22, 23]. In this paper, we start off with a first, yet essential task, which is to search for compact sets \mathcal{K} with non-empty interior that are strictly $\Gamma_{a,\theta}$ -invariant.

When looking for strictly $\Gamma_{a,\theta}$ -invariant sets \mathcal{K} , we will distinguish two types: if $\mathcal{F}(\mathcal{K}) \subseteq \mathcal{K}$, we will say that \mathcal{K} is *first-rate*, and *second-rate* otherwise.

Definition 7 A set $\mathcal{K} \subseteq \mathbb{R}^2$ is said to be *$A_{a,\theta}$ -self-similar* if $A_{a,\theta}(\mathcal{K}_0) = \mathcal{K}$, where $\mathcal{K}_0 = \{(x, y) \in \mathcal{K} : x \leq 1\}$.

Clearly, first-rate strictly $\Gamma_{a,\theta}$ -invariant sets are $A_{a,\theta}$ -self-similar. Therefore, in order to prove the existence of first-rate strictly $\Gamma_{a,\theta}$ -invariant sets we will prove the following result of existence of $A_{a,\theta}$ -self-similar sets.

Theorem A For every $(a, \theta) \in (1, \infty) \times (0, \pi)$, there exists a convex $(N+1)$ -sided polygon \mathcal{R}_N for some natural number $N = N(a, \theta) \geq 1 + \lfloor \pi/\theta \rfloor$ such that $\mathcal{K}_N := \Gamma_{a,\theta}(\mathcal{R}_N)$ is the maximal $A_{a,\theta}$ -self-similar set. Moreover, there exists a non-increasing sequence $(a_j)_j$ with the following properties:

- (a) $a_j \geq 1$ for every $j \in \mathbb{N}$.
- (b) For any $j \in \mathbb{N}$, $a_{j+1} \leq a_j$ with equality holding if and only if $a_j = 1$.
- (c) $\lim_{j \rightarrow \infty} a_j = 1$.
- (d) $\{a_j\}_j$ is finite if and only if $\frac{\theta}{\pi} \in \mathbb{Q}$.
- (e) The sequence $(N_j)_j$ with $N_j = N(a_j, \theta)$ is increasing.
- (f) For every $j \in \mathbb{N}$ and for all $a_j \leq a < a_{j-1}$ it holds that $N(a, \theta) = N_j$.

In practice, proving that \mathcal{K}_N is strictly invariant is reduced to checking that $\mathcal{F}(\mathcal{K}_N) \subseteq \mathcal{R}_N$. Since $A_{a,\theta}$ multiplies the area of any set by a factor of a^2 and \mathcal{F} at most halves it, it is clear that strictly invariant compact sets with non-empty interior can only exist for $a \leq \sqrt{2}$. This condition is not sufficient: if $a \leq \sqrt{2}$, then the $A_{a,\theta}$ -self-similar sets given in Theorem A are not necessarily strictly invariant. As an extreme example, for $\theta = 2\pi/3$ the $A_{a,\theta}$ -self-similar sets that exist for each $a > 1$ are triangles that are never strictly invariant. For $\theta = \pi/2$, however, all the self-similar polygons that exist are strictly invariant rectangles when $a \leq \sqrt{2}$. According to the next result, except for $\theta = 2\pi/3$, the $A_{a,\theta}$ -self-similar sets become strictly invariant as $a \rightarrow 1$.

Theorem B Let $\theta \in (0, \pi)$. If $\theta \neq 2\pi/3$, then there exists $a_\theta > 1$ such that $\mathcal{K}_{N(a)}$ is strictly $\Gamma_{a,\theta}$ -invariant for all $a \in (1, a_\theta]$.

Strictly invariant sets referred to in Theorem B are first-rate since they are self-similar. Second-rate strictly invariant sets do also exist, complicating the study of the dynamics of the family $\Gamma_{a,\theta}$. Some examples are provided for $\theta = 2\pi/3$.

This paper is organized as follows. In Section 2, we develop the construction of the maximal self-similar polygons of Theorem A and prove such theorem. Section 3 is devoted to studying when the self-similar sets seen in Section 2 are strictly invariant, and finally we prove Theorem B. In Section 4, second-rate strictly invariant sets are constructed for $\theta = 2\pi/3$. This work finishes with a brief Section 5 stating some open questions for future works, especially aiming for characterizing when a strictly invariant set \mathcal{K}_N is minimal (and, consequently, an attractor), and studying what other attractors it contains otherwise.

2 Existence of self-similar sets: the polygon \mathcal{K}_N

From now on, we will denote $\mathcal{C} = \{(x, y) \in \mathbb{R}^2 : x = 1\}$ and $\mathcal{O} = (0, 0)$. The aim of this section is to study the dynamics of the family of EBMs

$$\{\Gamma_{a,\theta} = \text{EBM}(\mathcal{C}, \mathcal{O}, A_{a,\theta}) : (a, \theta) \in \Delta\}$$

where $\Delta = (1, \infty) \times (0, \pi)$ and $A_{a,\theta}$ is the a -expanding counterclockwise 2-D rotation of angle θ . We will refer to this family as the *2-D tent maps family* and we will focus on the existence of strictly invariant compact sets for these *EBMs*. Recall that the attractors of $\Gamma_{a,\theta}$, provided that they exist, as well as their respective stable sets and their closure, are strictly $\Gamma_{a,\theta}$ -invariant. Moreover, attractors are compact and minimal (i.e. containing no non-empty compact strictly invariant set different from themselves), while the closure of their respective stable sets are maximal (i.e. contained in no strictly invariant set different from themselves).

In order to find strictly invariant sets, first we will search for self-similar sets. Let \mathcal{K} be a self-similar set. According to definition 7, $A_{a,\theta}(\mathcal{K}_0) = \mathcal{K}$ with \mathcal{K}_0 contained in $\Pi_0 = \{x \leq 1\}$. Since $\mathcal{K}_0 \subseteq \mathcal{K}$, then

$$\mathcal{K}_0 \subseteq \mathcal{K} = A_{a,\theta}(\mathcal{K}_0) \subseteq A_{a,\theta}(\Pi_0).$$

Setting $\Pi_n = A_{a,\theta}^n(\Pi_0)$ and

$$\mathcal{R}_n = \Pi_n \cap \Pi_{n-1} \cap \cdots \cap \Pi_0$$

for each $n \geq 0$, it holds that $\mathcal{K}_0 \subseteq \mathcal{R}_n$ for all n by induction. Therefore, every self similar set is contained in $A_{a,\theta}(\bigcap_{n=0}^{\infty} \mathcal{R}_n)$. We will prove that the latter set is an $A_{a,\theta}$ self-similar polygon.

Let $(a, \theta) \in \Delta$. For each $n \geq 0$, the line $\mathcal{L}_n = \mathcal{L}_n(a, \theta) = A_{a,\theta}^n(\mathcal{C})$ is implicitly given by the equation

$$\mathcal{L}_n \equiv x \cos n\theta + y \sin n\theta = a^n \tag{8}$$

so that the distance between \mathcal{L}_n and \mathcal{O} is equal to a^n and

$$\Pi_n = \{x \cos n\theta + y \sin n\theta \leq a^n\}.$$

From now on, unless otherwise stated, the angles $n\theta$ will be taken $\pmod{2\pi}$.

A line \mathcal{L}_n is vertical if and only if $\sin n\theta = 0$. Otherwise, its slope is equal to $-\cot n\theta$. In addition, two lines \mathcal{L}_n and \mathcal{L}_m are parallel if and only if $\sin(n-m)\theta = 0$. Otherwise, they intersect at the point

$$\mathcal{V}_{n,m} = \mathcal{V}_{n,m}(a, \theta) = (x_{n,m}, y_{n,m}) \quad (9)$$

with

$$\begin{aligned} x_{n,m} &= x_{n,m}(a, \theta) = (a^m \sin n\theta - a^n \sin m\theta) \csc(n-m)\theta, \\ y_{n,m} &= y_{n,m}(a, \theta) = (a^m \cos n\theta - a^n \cos m\theta) \csc(m-n)\theta. \end{aligned}$$

Note that $A_{a,\theta}^\ell(\mathcal{V}_{n,m}) = \mathcal{V}_{n+\ell,m+\ell}$ for every $\ell \geq 0$ whenever $\mathcal{V}_{n,m}$ exists.

In the following proposition, whose proof is straightforward, we show that there exists a natural number N such that $\mathcal{R}_N = \mathcal{R}_n$ for all $n \geq N$.

Proposition 1 *The following statements hold for any $(a, \theta) \in \Delta$:*

- (a) *The sequence of sets $\{\mathcal{R}_n\}_n$ is non-increasing (with respect to inclusion) and bounded below by the closed unit disc. In addition, \mathcal{R}_n is a (possibly unbounded) closed convex polygon.*
- (b) *Let $N_\theta = 1 + \lfloor \frac{\pi}{\theta} \rfloor$, where $\lfloor \cdot \rfloor$ denotes the floor function. Then,*

$$\theta \leq (N_\theta - 1)\theta \leq \pi < N_\theta\theta \leq \pi + \theta.$$

In particular,

- (i) $2 \leq N_\theta < \frac{2\pi}{\theta}$ and $\sin N_\theta\theta < 0$,
 - (ii) $N_\theta = \min\{n \in \mathbb{N} : \theta > \frac{\pi}{n}\}$,
 - (iii) $N_\theta = \min\{n \in \mathbb{N} : \mathcal{R}_n \text{ is bounded}\}$.
- (c) *For any $n \in \mathbb{N}$ it holds that $\mathcal{R}_n = \mathcal{R}_{n+1}$ if and only if $\mathcal{L}_{n+1} \cap \text{int } \mathcal{R}_n = \emptyset$.*
- (d) *There exists n such that $\mathcal{R}_n = \mathcal{R}_{n+1}$. Letting*

$$N = N(a, \theta) = \inf\{n \in \mathbb{N} : \mathcal{R}_n = \mathcal{R}_{n+1}\},$$

then $\mathcal{R}_N = \bigcap_{n=0}^{\infty} \Pi_n$.

- (e) $N \geq N_\theta$ with equality holding if and only if $\min\{x_{N_\theta, N_\theta+1}, x_{1, N_\theta+1}\} \geq 1$.

Remark 2 The definition of the natural number N given at statement d can be extended to the limit case $a = 1$ for every angle $\theta \in (0, \pi)$ enjoying the same properties, except maybe for the finiteness. In this case, the map $A_{1,\theta}$ is non-expansive, so $\Gamma_{1,\theta}$ is no longer an *EBM*. It is easy to check that

$$N(1, \theta) = \inf\{n : \cos(n+1)\theta = 1\} \in \{1, 2, \dots, \infty\}.$$

Let us write $\theta = 2\pi\beta$. If $\beta = \frac{p}{q} \in \mathbb{Q}$ with p and q coprime, then $N(1, \theta) = q-1$ and \mathcal{R}_{q-1} is a regular q -sided polygon centered at the origin. On the other hand, if β is an irrational number, then $N(1, \theta) = \infty$ and \mathcal{R}_∞ is the closed unit disc.

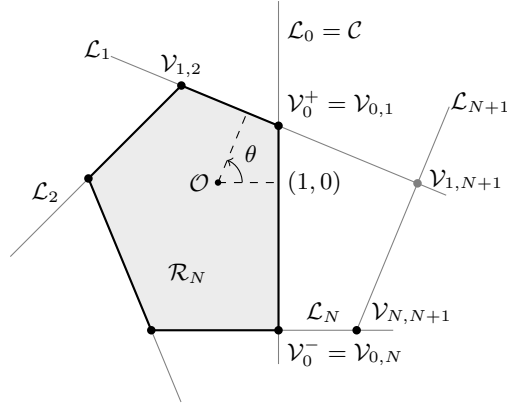


Fig. 1: The polygon \mathcal{R}_N (with $N = 4$) for $a = 1.25$ and $\theta = \frac{3\pi}{8}$

The limit case $a = 1$ is of little interest to us since $\mathcal{R}_{N(1,\theta)}$ is strictly $\Gamma_{1,\theta}$ -invariant for all θ , but cannot be a strange attractor. However, in the rational case, the natural number $N(1,\theta)$ from Remark 2 proves to be useful as it is a non-trivial upper bound for N because $\mathcal{L}_{N(1,\theta)+1}(a) \cap \text{int } \mathcal{R}_{N(1,\theta)}(a) = \emptyset$ for every a . This implies, in particular, that $N(a, \frac{2\pi}{3}) = 2$ and $N(a, \frac{\pi}{2}) = 3$ for all a .

The $(N+1)$ -sided convex polygon \mathcal{R}_N , limited by the lines $\mathcal{L}_0, \mathcal{L}_1, \dots, \mathcal{L}_N$, will be the core of our candidate for the maximal strictly $\Gamma_{a,\theta}$ -invariant set, which will be none other than its image under $A_{a,\theta}$. For simplicity, let us now introduce the following notation:

- $\mathcal{V}_0^+ = \mathcal{V}_0^+(a, \theta)$ and $\mathcal{V}_0^- = \mathcal{V}_0^-(a, \theta)$ denote the upper and lower vertices of \mathcal{R}_N on \mathcal{L}_0 , respectively, see Figure 1.
- $n^\pm = n^\pm(a, \theta)$ denote the unique natural numbers such that $\mathcal{V}_0^+ = \mathcal{V}_{0,n^+}$ and $\mathcal{V}_0^- = \mathcal{V}_{0,n^-}$. Note that $n^\pm \in \{1, 2, \dots, N\}$. Moreover, $\sin n^+\theta > 0$ and $\sin n^-\theta < 0$ since $y_0^+ > 0$ and $y_0^- < 0$, respectively, see (9).
- $\mathcal{O}_0^+ = \mathcal{O}_0^+(a, \theta)$ and $\mathcal{O}_0^- = \mathcal{O}_0^-(a, \theta)$ denote the $A_{a,\theta}$ -orbits on \mathcal{R}_N of \mathcal{V}_0^+ and \mathcal{V}_0^- , respectively. These orbits lie on the boundary $\partial\mathcal{R}_N$ of \mathcal{R}_N and consist of a finite number of points.
- $\ell^\pm = \ell^\pm(a, \theta)$ denote the lengths of \mathcal{O}_0^+ and \mathcal{O}_0^- . Note that $\ell^\pm(a, \theta) \in \{1, 2, \dots, N+1\}$. Moreover, $\mathcal{O}_0^\pm = \{\mathcal{V}_{\ell, \ell+n^\pm}\}_{\ell=0}^{\ell^\pm-1}$.

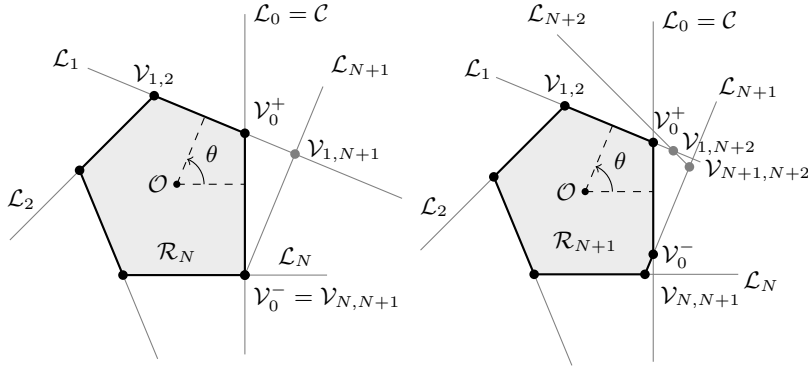
These numbers will play a crucial role in what follows.

For example, if $N < \frac{2\pi}{\theta}$ (e.g. for $N = N_\theta$), the $N+1$ vertices of \mathcal{R}_N are $\mathcal{V}_{0,1}, \mathcal{V}_{1,2}, \dots, \mathcal{V}_{N-1,N}$, and $\mathcal{V}_{0,N}$. In particular, $n^+ = 1$ and $n^- = N$ (see Figure 1).

As a consequence of the definition of the sequence $\{\mathcal{R}_n\}_n$, the following result holds.

Proposition 2 For every $(a, \theta) \in \Delta$, the $N+1$ vertices of \mathcal{R}_N are $\mathcal{O}_0^+ \cup \mathcal{O}_0^-$. Moreover, one and only one of the following three statements holds:

- (a) $\mathcal{L}_{N+1} \cap \partial\mathcal{R}_N = \emptyset$ and $\mathcal{O}_0^+ \cap \mathcal{O}_0^- = \emptyset$.
- (b) $\mathcal{L}_{N+1} \cap \partial\mathcal{R}_N = \{\mathcal{V}_0^+\}$ and $\mathcal{O}_0^+ \cup \mathcal{O}_0^- = \mathcal{O}_0^-$.
- (c) $\mathcal{L}_{N+1} \cap \partial\mathcal{R}_N = \{\mathcal{V}_0^-\}$ and $\mathcal{O}_0^+ \cup \mathcal{O}_0^- = \mathcal{O}_0^+$.



(a) The polygon \mathcal{R}_4 for $a = 1.074\dots$ (b) The polygon \mathcal{R}_5 for $a \lesssim 1.074\dots$

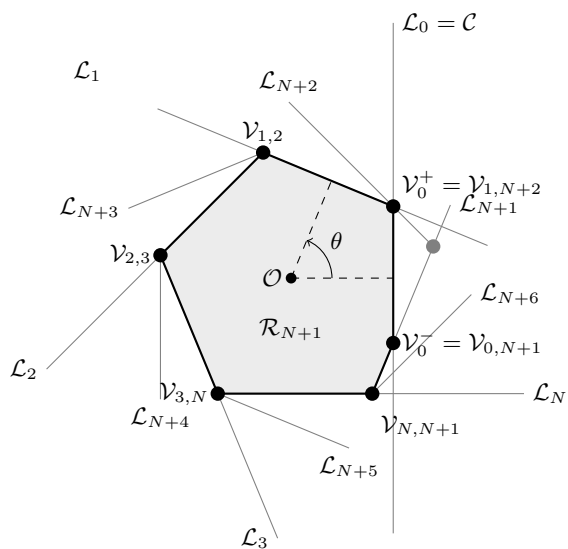
Fig. 2: Bifurcation from \mathcal{V}_0^- for $\theta = \frac{3\pi}{8}$

We will prove Proposition 2 later on. According to it, essentially only two scenarios can take place:

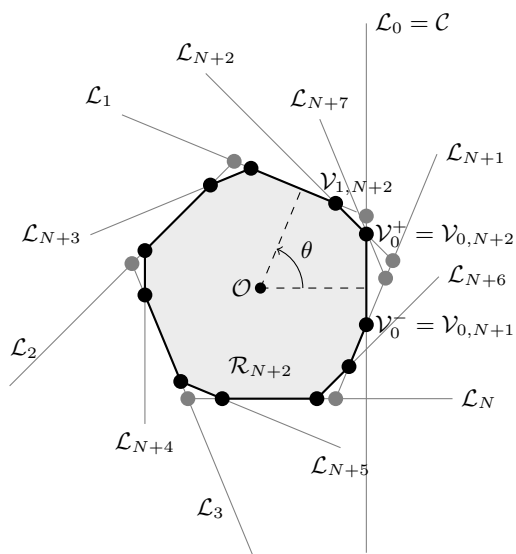
- (i) If the line \mathcal{L}_{N+1} comes into contact with \mathcal{R}_N at either \mathcal{V}_0^+ or \mathcal{V}_0^- , then the orbit of the contact vertex \mathcal{V}_0^σ , with $\sigma = +$ or $\sigma = -$, is strictly contained in the orbit of the other one, which thus runs through all the vertices of \mathcal{R}_N .
- (ii) If the line \mathcal{L}_{N+1} does not intersect \mathcal{R}_N at all, then \mathcal{V}_0^+ or \mathcal{V}_0^- have disjoint orbits whose union consist of all the vertices of \mathcal{R}_N .

Note that, if the line \mathcal{L}_{N+1} does not intersect \mathcal{R}_N , the structure of \mathcal{R}_N is persistent in the sense that the corresponding perturbed polygon $\mathcal{R}_{N(\tilde{a},\theta)}(\tilde{a},\theta)$ with $\tilde{a} = a + \varepsilon$ for every sufficiently small $|\varepsilon|$ is essentially the same as \mathcal{R}_N (in particular, they have the same number of sides). Otherwise, this is not so for $\varepsilon < 0$, where a bifurcation occurs on the boundary of \mathcal{R}_N : each and every vertex in the orbit of the contact vertex \mathcal{V}_0^σ bifurcates into two new ones giving rise to a polygon with $N(a) + \ell^\sigma(a) + 1$ sides (see Figures 2-3). We will carry out a study of this bifurcation process later.

We can firstly consider the non-expansive case $a = 1$ in order to understand this process. In this case, if $\theta = 2\pi\frac{p}{q}$, then $N = q - 1$ and \mathcal{R}_N is limited by



(a) The polygon \mathcal{R}_5 for $a = 1.031\dots$



(b) The polygon \mathcal{R}_{10} for $a \lesssim 1.031\dots$

Fig. 3: Bifurcation from v_0^+ for $\theta = \frac{3\pi}{8}$

the lines $\mathcal{L}_1, \mathcal{L}_2, \dots, \mathcal{L}_q = \mathcal{L}_0$, which are tangent to the unit circle at $e^{i\theta_k}$ with

$\theta_k = 2k\pi\frac{p}{q}$ for $k = 0, 1, \dots, q-1$. The orbit $\{e^{i\theta_k}\}_{k=1}^q$ is not necessarily ordered along the circle. Denote $0 < \theta_r < \theta_s < 2\pi$ the contiguous angles to $\theta = 0$. If $a = 1$ then the polygon \mathcal{R}_N is regular and it is contained in Π_0 . However, if $a = 1 + \varepsilon$ then the line \mathcal{L}_q is the vertical line $x = (1 + \varepsilon)^q > 1$. By considering ε small enough so that $(1 + \varepsilon)^r \cos \theta_r < 1$ and $(1 + \varepsilon)^s \cos \theta_s < 1$, then \mathcal{R}_N continues to be a polygon with q sides limited by the lines $\mathcal{L}_1, \mathcal{L}_2, \dots, \mathcal{L}_q, \mathcal{L}_0$. Otherwise, the polygon \mathcal{R}_N has $N + 1 < q$ sides. In fact, the number of sides of \mathcal{R}_N remains constant or decreases as a increases until \mathcal{R}_N becomes a primary polygon according to the following definition.

Definition 8 A polygon \mathcal{R}_N is said to be *primary* if $N = N_\theta$, i.e., if \mathcal{R}_N has $N_\theta + 1$ sides.

A primary polygon has the minimum number of sides $N_\theta + 1$ and it is clearly obtained for a large enough. As a decreases towards $a = 1$, the number of sides $N + 1$ increases to q if $\theta = 2\pi\frac{p}{q}$ or it tends to infinity if $\frac{\theta}{\pi} \notin \mathbb{Q}$.

Fixed $\theta \in (0, \pi)$, next we will study the variation of N with respect to a . According to the construction of \mathcal{R}_N it is clear that $N = N(a, \theta)$ remains constant until a certain value of a for which the line \mathcal{L}_{N+1} intersects \mathcal{R}_N at a vertex $\mathcal{V}_0^+(a, \theta)$ or $\mathcal{V}_0^-(a, \theta)$ on the line \mathcal{L}_0 . These values of a for which the natural number N changes we will be called the *bifurcation values*. Just to clarify these ideas, for each $\theta \in (0, \pi)$ let us consider the map

$$a \in [1, \infty) \mapsto N(a, \theta) \in \mathbb{N}. \quad (10)$$

We will indirectly prove that this map is non-increasing and piecewise constant. Of course, its points of discontinuity will be precisely the bifurcation values associated to θ . We advance that each bifurcation sequence will be decreasingly convergent to 1 for every $\theta \in (0, \pi)$. We will meet two different situations:

- (i) If $\frac{\theta}{\pi} \in \mathbb{Q}$, then the set of points of discontinuity of the map given in (10) is finite. In this case, the bifurcation sequence is eventually constant equal to 1.
- (ii) If $\frac{\theta}{\pi} \notin \mathbb{Q}$, then the set of points of discontinuity of the map given in (10) is countably infinite and accumulates at 1.

Of course, the irrational case shows much more dynamical richness than the rational one, nonetheless keeping in mind that the map given in (10) is always non-increasing. In both cases, and once the value of θ is fixed, the domain of definition of this map can be decomposed as the (finite or infinite) disjoint union of intervals on which it will be continuous (i.e. constant). Our aim is to determine, at once, the bifurcation sequence and the value of the map given in (10) on such intervals.

The proof of Proposition 2 will be straightforward by the following lemma:

Lemma 1 *The following statements hold for every $(a, \theta) \in \Delta$:*

- (a) *If $\mathcal{V}_{n,m}$ is a vertex of \mathcal{R}_N , then either $|n - m| = n^+$ or $|n - m| = n^-$.*

- (b) If $\mathcal{V}_{n,m}$ is a vertex of \mathcal{R}_N , then $\mathcal{V}_{n+1,m+1}$ is a vertex of \mathcal{R}_N if and only if $x_{n+1,m+1} \leq 1$.
- (c) $\ell^\pm = \min\{\ell \in \mathbb{N} : x_{\ell,\ell+n^\pm} > 1\}$ for all $a > 1$.
- (d) $\mathcal{O}_0^\pm \subset \mathcal{O}_0^\mp$ if and only if $\mathcal{V}_0^\pm \in \mathcal{O}_0^\mp$.
- (e) $\mathcal{O}_0^+ \cap \mathcal{O}_0^- \neq \emptyset$ if and only if either $\mathcal{V}_0^+ \in \mathcal{O}_0^-$ or $\mathcal{V}_0^- \in \mathcal{O}_0^+$.
- (f) $\mathcal{L}_{N+1} \cap \partial\mathcal{R}_N \neq \emptyset$ if and only if either $\mathcal{V}_0^+ \in \mathcal{L}_{N+1}$ or $\mathcal{V}_0^- \in \mathcal{L}_{N+1}$.
- (g) If $\mathcal{V}_0^\pm \in \mathcal{L}_{N+1}$, then $\mathcal{V}_0^\pm \in \mathcal{O}_0^\mp$.
- (h) If $\mathcal{L}_{N+1} \cap \partial\mathcal{R}_N = \emptyset$, then $\mathcal{O}_0^+ \cap \mathcal{O}_0^- = \emptyset$.

Proof (Proposition 2) Let $\mathcal{V}_{n,m}$ be a vertex of \mathcal{R}_N with $n < m$. Then, either $\mathcal{V}_{0,m-n} = \mathcal{V}_0^+$ or $\mathcal{V}_{0,m-n} = \mathcal{V}_0^-$, so either $\mathcal{V}_{n,m} = A_{a,\theta}^n(\mathcal{V}_0^+)$ or $\mathcal{V}_{n,m} = A_{a,\theta}^n(\mathcal{V}_0^-)$, and therefore $\mathcal{V}_{m,n} \in \mathcal{O}_0^+ \cup \mathcal{O}_0^-$. The rest is obvious by Lemma 1. ■

We end this subsection by introducing an important polygon.

Proposition 3 *The following statements hold for every $(a, \theta) \in \Delta$:*

- (a) *The set $\mathcal{K}_N = A_{a,\theta}(\mathcal{R}_N)$ is the convex $(N+1)$ -sided polygon limited by the lines $\mathcal{L}_1, \mathcal{L}_2, \dots, \mathcal{L}_{N+1}$. The two vertices of \mathcal{K}_N on \mathcal{L}_{N+1} are \mathcal{V}_{N+1,n^+} and \mathcal{V}_{N+1,n^-} . These vertices, located on the half-plane $\{x \geq 1\}$, are called the proper vertices of \mathcal{K}_N and are denoted by \mathcal{V}_{N+1}^+ and \mathcal{V}_{N+1}^- , respectively.*
- (b) *The polygon \mathcal{K}_N is $A_{a,\theta}$ -self-similar.*
- (c) *Every $A_{a,\theta}$ -self-similar set is contained in \mathcal{K}_N . In particular, if \mathcal{K}_N is strictly $\Gamma_{a,\theta}$ -invariant itself, then it is the maximal first-rate strictly $\Gamma_{a,\theta}$ -invariant set.*

Proof (a) Clear by construction.

(b) From statements a and c of Proposition 1 it follows that

$$\mathcal{K}_N \cap \mathcal{R}_N = \mathcal{R}_{N+1} = \mathcal{R}_N,$$

so that \mathcal{R}_N is contained in \mathcal{K}_N .

(c) Let \mathcal{K} be a $A_{a,\theta}$ -self-similar set, and let $\mathcal{K}_0 = \mathcal{K} \cap \{x \leq 1\}$. It is clear that $\mathcal{K}_0 \subset \Pi_0$. Proceeding by induction, if we assume that $\mathcal{K}_0 \subset \Pi_n$, then

$$\mathcal{K}_0 \subseteq \mathcal{K} = A_{a,\theta}(\mathcal{K}_0) \subset A_{a,\theta}(\Pi_n) = \Pi_{n+1}.$$

so that $\mathcal{K}_0 \subseteq \mathcal{R}_N$ by statement d of Proposition 1, and therefore $\mathcal{K} = A_{a,\theta}(\mathcal{K}_0) \subseteq \mathcal{K}_N$. ■

Corollary 1 *Every first-rate strictly invariant set is bounded.*

2.1 The bifurcation sequence

For each fixed angle $\theta \in (0, \pi)$, the respective bifurcations (if any) occur at those values $a_j = a_j(\theta)$ for which the line \mathcal{L}_{N_j+1} contains either of the vertices \mathcal{V}_{0,n_j^+} or \mathcal{V}_{0,n_j^-} that the polygon \mathcal{R}_{N_j} has on the critical line $\mathcal{L}_0 = \mathcal{C}$. For

a slightly less than a_j , another polygon with $N_{j+1} + 1$ sides appears, where $N_{j+1} = N_j + \ell_j^+$ or $N_{j+1} = N_j + \ell_j^-$ depending on whether the contact takes place at \mathcal{V}_{0,n_j^+} or \mathcal{V}_{0,n_j^-} , respectively. Recall that ℓ_j^+ and ℓ_j^- denote the lengths of the orbits of \mathcal{V}_{0,n_j^+} and \mathcal{V}_{0,n_j^-} , respectively. Therefore, in order to determine the sequence of bifurcation values a_j in an iterative way, we define the 6-tuple

$$\mathcal{A}_j = \mathcal{A}_j(\theta) = (a_j, N_j, n_j^+, n_j^-, \ell_j^+, \ell_j^-),$$

that we call a *bifurcation stair-step*. Each \mathcal{A}_j is a tag representing a $(N_j + 1)$ -sided bounded polygon that becomes a $(N_{j+1} + 1)$ -sided bounded polygon for $a \lesssim a_j$.

The largest bifurcation value a_1 is associated to the primary polygon \mathcal{R}_{N_θ} , see Proposition 1. For this polygon we have $N_1 = N_\theta$, $n_1^+ = \ell_1^- = 1$ and $n_1^- = \ell_1^+ = N_\theta$. Therefore, the first bifurcation stair-step is

$$\mathcal{A}_1 = (a_1, N_\theta, 1, N_\theta, N_\theta, 1).$$

where a_1 depends on $\sigma_1 = \text{sgn}(\sin(N_\theta + 1)\theta)$:

- If $\sigma_1 = 0$, then the line $\mathcal{L}_{N_\theta+1}(a)$ is vertical for all $a \geq 1$, so no bifurcation occurs and $a_1 = 1$. Note that $\sigma_1 = 0$ if and only if $\theta \in \{\frac{\pi}{2}, \frac{2\pi}{3}\}$.
- If $\sigma_1 = +1$, the upper vertex is $\mathcal{V}_{0,1}(a_1) = (1, (a_1 - \cos \theta) \csc \theta)$, see (9), and the line $\mathcal{L}_{N_\theta+1}(a_1)$ is given by

$$x \cos(N_\theta + 1)\theta + y \sin(N_\theta + 1)\theta = a_1^{N_\theta+1},$$

see (8). Since $\mathcal{V}_{0,1}(a_1) \in \mathcal{L}_{N_\theta+1}(a_1)$, it holds that

$$a_1^{N_\theta+1} \sin \theta - a_1 \sin(N_\theta + 1)\theta + \sin N_\theta \theta = 0. \quad (11)$$

- If $\sigma_1 = -1$, the lower vertex is $\mathcal{V}_{0,N_\theta}(a_1) = (1, (a_1^{N_\theta} - \cos N_\theta \theta) \csc N_\theta \theta)$, see (9). Since $\mathcal{V}_{0,N_\theta}(a_1) \in \mathcal{L}_{N_\theta+1}(a_1)$, it holds that

$$a_1^{N_\theta+1} \sin N_\theta \theta - a_1^{N_\theta} \sin(N_\theta + 1)\theta + \sin \theta = 0. \quad (12)$$

Equations (11) and (12) can be seen as polynomials of the form

$$\begin{aligned} p_1^+(a) &= a^{r_1+s_1} \sin r_1 \theta - a^{r_1} \sin(r_1 + s_1)\theta + \sin s_1 \theta, \\ p_1^-(a) &= a^{r_1+s_1} \sin s_1 \theta - a^{s_1} \sin(r_1 + s_1)\theta + \sin r_1 \theta, \end{aligned}$$

where $r_1 = 1$ and $s_1 = N_\theta$. In the following lemma we prove that these polynomials have unique positive roots denoted by a_1^+ and a_1^- , respectively. Then, it holds that $a_1 = \max\{a_1^+, a_1^-\}$.

Lemma 2 *Let $\theta \in (0, \pi)$, and let $r, s \in \mathbb{N}$ such that $\sin r\theta > 0$ and $\sin s\theta < 0$. Then, the polynomials*

$$\begin{aligned} p^+(a) &= a^{r+s} \sin r\theta - a^r \sin(r+s)\theta + \sin s\theta, \\ p^-(a) &= a^{r+s} \sin s\theta - a^s \sin(r+s)\theta + \sin r\theta, \end{aligned}$$

have unique positive roots $a^+ = a^+(\theta)$ and $a^- = a^-(\theta)$, respectively. Moreover, the roots a^+ and a^- are simple and $a^+ \cdot a^- = 1$.

Proof The existence and uniqueness of a^+ and a^- are guaranteed by Descartes' rule of signs as $\sin r\theta > 0$ and $\sin s\theta < 0$. Moreover, since $p^-(a)$ is the reciprocal polynomial of $p^+(a)$, then $a^- = \frac{1}{a^+}$ by uniqueness. ■

The construction of the bifurcation sequence is iteratively obtained from \mathcal{A}_1 according to the following result. For each $j \in \mathbb{N}$, let us denote

$$\sigma_j = \text{sgn}(\sin(N_j + 1)\theta) .$$

Proposition 4 *For every $j \in \mathbb{N}$, given*

$$\mathcal{A}_j = (a_j, N_j, n_j^+, n_j^-, \ell_j^+, \ell_j^-),$$

the next bifurcation stair-step

$$\mathcal{A}_{j+1} = (a_{j+1}, N_{j+1}, n_{j+1}^+, n_{j+1}^-, \ell_{j+1}^+, \ell_{j+1}^-)$$

is obtained applying the following rule:

(a) *Case $\sigma_j = +1$:*

$$N_{j+1} = N_j + \ell_j^+, \quad n_{j+1}^+ = \ell_{j+1}^- = N_j + 1, \quad n_{j+1}^- = n_j^-, \quad \ell_{j+1}^+ = \ell_j^+.$$

(b) *Case $\sigma_j = -1$:*

$$N_{j+1} = N_j + \ell_j^-, \quad n_{j+1}^+ = n_j^+, \quad n_{j+1}^- = \ell_{j+1}^+ = N_j + 1, \quad \ell_{j+1}^- = \ell_j^-.$$

(c) *Case $\sigma_j = 0$:*

$$N_{j+1} = N_j, \quad n_{j+1}^+ = n_j^+, \quad n_{j+1}^- = n_j^-, \quad \ell_{j+1}^+ = \ell_j^+, \quad \ell_{j+1}^- = \ell_j^-.$$

In order to obtain a_{j+1} , if $\sigma_{j+1} = 0$, then $a_{j+1} = 1$. Otherwise, the bifurcation value a_{j+1} is the unique positive root of the polynomial

$$p_{j+1}^+(a) = a^{N_{j+1}+1} \sin n_{j+1}^+ \theta - a^{n_{j+1}^+} \sin(N_{j+1} + 1)\theta + \sin n_{j+1}^- \theta$$

if $\sigma_{j+1} = +1$, or of

$$p_{j+1}^-(a) = a^{N_{j+1}+1} \sin n_{j+1}^- \theta - a^{n_{j+1}^-} \sin(N_{j+1} + 1)\theta + \sin n_{j+1}^+ \theta$$

if $\sigma_{j+1} = -1$, respectively.

Proof If $\sigma_j = 0$, then the line $\mathcal{L}_{N_{j+1}}(a)$ is vertical for all $1 \leq a < a_{j-1}$, so no other bifurcation occurs. Therefore, all parameters of \mathcal{A}_j remain constant and $a_j = 1$. If $\sigma_j \neq 0$, then from our geometric discussion in the previous subsection we deduce the values of the entries of \mathcal{A}_{j+1} . In this case, if $\sigma_{j+1} = +1$, then the upper vertex

$$\mathcal{V}_0^+(a_{j+1}) = (1, (a_{j+1}^{n_{j+1}^+} - \cos n_{j+1}^+ \theta) \csc n_{j+1}^+ \theta), \quad (13)$$

see (9), belongs to the line $\mathcal{L}_{N_{j+1}+1}(a_{j+1})$, whose equation is

$$x \cos(N_{j+1} + 1)\theta + y \sin(N_{j+1} + 1)\theta = a_{j+1}^{N_{j+1}+1}, \quad (14)$$

see (8). From a direct substitution of (13) into (14) we obtain $p_{j+1}^+(a_{j+1}) = 0$. Similarly, if $\sigma_{j+1} = -1$, then the lower vertex

$$\mathcal{V}_0^-(a_{j+1}) = (1, (a_{j+1}^{n_{j+1}^-} - \cos n_{j+1}^- \theta) \csc n_{j+1}^- \theta), \quad (15)$$

see (9), belongs to the line $\mathcal{L}_{N_{j+1}+1}(a_{j+1})$. From a direct substitution of (15) into (14) we obtain $p_{j+1}^-(a_{j+1}) = 0$.

The uniqueness of the positive roots of $p_{j+1}^+(a)$ and $p_{j+1}^-(a)$ is due to Lemma 2. \blacksquare

The result that we prove next contains Theorem A.

Theorem 1 *For every $\theta \in (0, \pi)$ there exists a non-increasing sequence $(a_j)_j$, called the bifurcation sequence, with the following properties:*

- (a) $a_j \geq 1$ for every $j \in \mathbb{N}$.
- (b) $\sigma_j = 0$ if and only if $a_j = 1$ for every $j \in \mathbb{N}$.
- (c) For any $j \in \mathbb{N}$, $a_{j+1} \leq a_j$ with equality holding if and only if $a_j = 1$.
- (d) $\lim_{j \rightarrow \infty} a_j = 1$.
- (e) $\{a_j\}$ is finite if and only if $\frac{\theta}{\pi} \in \mathbb{Q}$.
- (f) The following statements hold for every $j \in \mathbb{N}$:
 - For every $a_j \leq a < a_{j-1}$, $N(a, \theta) = N_j$, $n^+(a, \theta) = n_j^+$ and $n^-(a, \theta) = n_j^-$. Moreover,

$$\mathcal{V}_{N+1, n^{\sigma_j}}(a_j) = \mathcal{V}_0^{\sigma_j}(a_j) = \mathcal{V}_{0, N+1}(a_j).$$

- For every $a_{j+1} < a \leq a_j$, $\ell^+(a, \theta) = \ell_j^+$ and $\ell^-(a, \theta) = \ell_j^-$.

Proof The first five statements hold as we have already discussed (see also Remark 2). We prove the last one by induction:

The case $j = 1$ is true by our previous results. Assume that this theorem holds for $j = k$ and let us prove it for $j = k + 1$. Assume without loss of generality that $\sigma_k = +1$. As we diminish the value of a from a_k to a_{k+1} , each point in the $A_{a_k, \theta}$ -orbit of $\mathcal{V}_0^+(a_k)$ bifurcates into two new ones, one in the $A_{a, \theta}$ -orbit of $\mathcal{V}_0^+(a)$ and the other in the $A_{a, \theta}$ -orbit of $\mathcal{V}_0^-(a)$, and this structure persists until the next contact takes place for $a = a_{k+1}$. It is easily deduced that for every $a_{k+1} \leq a < a_k$,

$$N(a) = N(a_k) + \ell^+(a_k) = N_k + \ell_k^+ = N_{k+1},$$

and

$$n^+(a) = N(a_k) + 1 = N_k + 1 = n_{k+1}^+$$

and

$$n^-(a) = n_k^- = n_{k+1}^-.$$

Now, if $a_{k+1} < a$, then

$$\ell^+(a) = \ell^+(a_k) = \ell_k^+$$

and

$$\ell^-(a) = \ell^-(a_k) = N_k + 1 = \ell_k^-.$$

Finally, if $\sigma_{k+1} \neq 0$, then

$$\ell^{\sigma_{k+1}}(a_{k+1}) = \ell_k^{\sigma_{k+1}} = \ell_{k+1}^{\sigma_{k+1}}$$

and

$$\ell^{-\sigma_{k+1}}(a_{k+1}) = N_{k+1} + 1 = \ell_{k+1}^{-\sigma_{k+1}}.$$

■

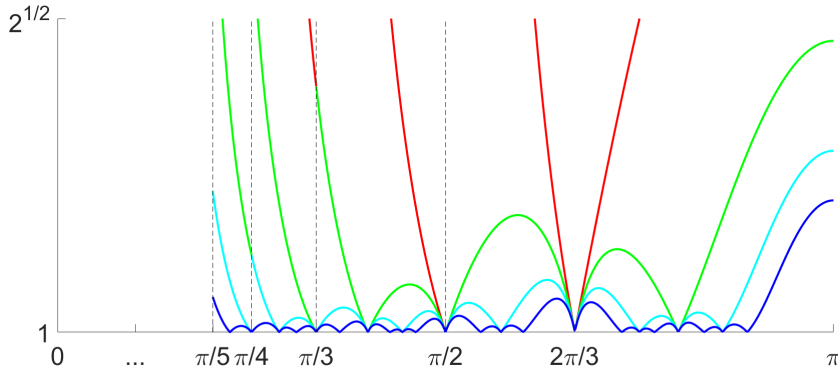


Fig. 4: The curves of the bifurcation values $a_j(\theta)$ for $j = 1$ (red), 2 (green), 3 (cyan), 4 (blue) and $\theta \in (\frac{\pi}{5}, \pi)$

We say that $a > 1$ is a *generic value* if it is not a bifurcation value. In Figure 4 we show a numerical approximation of the first bifurcation curves. The concatenation of some of them at certain points are justified by the following analytical results.

Proposition 5 For every $j \in \mathbb{N}$ it holds that $\sigma_j \equiv -1$ on $(0, \pi/(j+1))$.

Proof The result easily follows for $j = 1$. Assume that it holds for $j \leq k$ and let us prove it for $j = k+1$. Fix $\theta \in (0, \pi/(k+2))$. Since

$$(0, \pi/(k+2)) \subset (0, \pi/(k+1)) \subset \dots \subset (0, \pi/2),$$

then $\sigma_n(\theta) = -1$ for $n = 1, 2, \dots, k$ by the induction hypothesis, so $N_{k+1} + 1 = N_\theta + k + 1$. Note that $N_\theta \geq k + 3$. Now, since $\pi/N_\theta < \theta \leq \pi/(N_\theta - 1)$ if $N_\theta > k + 3$ and $\pi/N_\theta < \theta < \pi/(N_\theta - 1)$ if $N_\theta = k + 3$, then

$$\pi < \pi + \frac{(k+1)\pi}{N_\theta} < (N_{k+1} + 1)\theta \leq \pi + \frac{(k+2)\pi}{N_\theta - 1} < 2\pi,$$

so $\sigma_{k+1}(\theta) = -1$. ■

Corollary 2 *Let $j \in \mathbb{N}$. For all $k > j$, it holds that*

$$\lim_{\theta \downarrow \frac{\pi}{k}} a_j(\theta) = a_{j-1}\left(\frac{\pi}{k}\right).$$

3 Existence of first-rate strictly invariant sets

In the previous section we have seen that, for every $(a, \theta) \in \Delta$, the $(N + 1)$ -sided polygon $\mathcal{K}_N = II_{N+1} \cap II_N \cap \dots \cap II_1$ is the maximal $A_{a,\theta}$ -self-similar set. However, it may not be strictly $\Gamma_{a,\theta}$ -invariant. Two particular cases are $\theta = \frac{\pi}{2}$ and by $\theta = \frac{2\pi}{3}$. If $\theta = \frac{\pi}{2}$, then the respective self-similar rectangle is strictly invariant if and only if $a \leq \sqrt{2}$. On the other hand, if $\theta = \frac{2\pi}{3}$, then the respective self-similar triangle is strictly invariant if and only if $a = 1$. Recall that, for any $(a, \theta) \in \Delta$, if \mathcal{K}_N is strictly invariant, then $a \leq \sqrt{2}$ because \mathcal{K}_N is compact and has non-empty interior.

From the convexity of \mathcal{R}_N , it follows that \mathcal{K}_N is strictly invariant if and only if \mathcal{R}_N contains the images $\tilde{\mathcal{V}}_{N+1}^+$ and $\tilde{\mathcal{V}}_{N+1}^-$ under the fold of the proper vertices \mathcal{V}_{N+1}^+ and \mathcal{V}_{N+1}^- of \mathcal{K}_N , respectively. Computing the coordinates of these vertices and considering the equations of the lines \mathcal{L}_n , see (8) and (9), we obtain the following result:

Proposition 6 *For any $(a, \theta) \in \Delta$, the self-similar polygon \mathcal{K}_N is strictly invariant if and only if*

$$\begin{aligned} a^{N+1} \sin(n + n^+) \theta - a^{n^+} \sin(N + 1 + n) \theta - (a^n - 2 \cos n \theta) \sin n^- \theta &\geq 0 \\ a^{N+1} \sin(n + n^-) \theta - a^{n^-} \sin(N + 1 + n) \theta - (a^n - 2 \cos n \theta) \sin n^+ \theta &\geq 0 \end{aligned} \quad (16)$$

for all $n \in \{0, 1, \dots, N\}$.

Proof The proper vertices of \mathcal{K}_N are located on the right side of the critical line, so the result trivially follows for $n = 0$.

Let us now recall that the coordinates of the proper vertices of \mathcal{K}_N are

$$\begin{aligned} x_{n^\pm, N+1} &= (-a^{N+1} \sin n^\pm \theta + a^{n^\pm} \sin(N + 1) \theta) \csc n^\mp \theta \\ y_{n^\pm, N+1} &= (a^{N+1} \cos n^\pm \theta - a^{n^\pm} \cos(N + 1) \theta) \csc n^\mp \theta. \end{aligned}$$

Therefore, the *folded proper vertices* $\tilde{\mathcal{V}}_{N+1}^+$ and $\tilde{\mathcal{V}}_{N+1}^-$ are

$$\tilde{\mathcal{V}}_{N+1}^\pm = (2 - x_{n^\pm, N+1}, y_{n^\pm, N+1})$$

Since $\mathcal{R}_N = \Pi_N \cap \dots \cap \Pi_1 \cap \Pi_0$, then $\tilde{\mathcal{V}}_{N+1}^+$ and $\tilde{\mathcal{V}}_{N+1}^-$ belong to \mathcal{R}_N if and only if $\tilde{\mathcal{V}}_{N+1}^+ \in \Pi_n$ and $\tilde{\mathcal{V}}_{N+1}^- \in \Pi_n$ for each $n = 1, \dots, N$, that is, if and only if

$$\begin{aligned} (2 - x_{n^+, N+1}) \cos n\theta + y_{n^+, N+1} \sin n\theta &\leq a^n \\ (2 - x_{n^-, N+1}) \cos n\theta + y_{n^-, N+1} \sin n\theta &\leq a^n. \end{aligned} \quad (17)$$

Since $\sin n^+\theta > 0$ and $\sin n^-\theta < 0$, we obtain (16). \blacksquare

Remark 3 It is sufficient to check the inequalities of Proposition 6 for those $n \in \{1, \dots, N\}$ such that $\cos n\theta < 0$.

The characterization provided by Proposition 6 of the strict invariance of the $(N+1)$ -sided polygon \mathcal{K}_N has little practical value when N is large. However, the following corollary allows us to easily discard those which cannot be strictly invariant from a basic geometric remark.

Proposition 7 *Let $\theta \in (0, \pi)$. Assume that $\mathcal{K}_{N(a)}$ is strictly invariant for some $a > 1$. Then, the following statements hold:*

- (a) *If a is a generic value, then $\min\{\cos n^+\theta, \cos n^-\theta\} \geq 0$.*
- (b) *If a is a bifurcation value, then*

$$\min\{\cos n^{-\sigma}\theta, \sigma \sin(2n^\sigma + n^{-\sigma})\theta\} \geq 0$$

where σ is the sign of $\sin(N+1)\theta$.

Proof (a) Assume that a is a generic value. Then, neither \mathcal{V}_0^+ nor \mathcal{V}_0^- is a vertex of \mathcal{K}_N and the lines \mathcal{L}_{n^+} and \mathcal{L}_{n^-} must have non-positive and non-negative slopes because $\tilde{\mathcal{V}}_{N+1}^+ \in \Pi_{n^+}$ and $\tilde{\mathcal{V}}_{N+1}^- \in \Pi_{n^-}$, respectively. Since these slopes are equal to $-\cot n^\pm\theta$, and since $\sin n^+\theta > 0$ and $\sin n^-\theta < 0$, this implies that $\cos n^+\theta \geq 0$ and $\cos n^-\theta \geq 0$.

(b) Assume that a is a bifurcation value. Then, $\tilde{\mathcal{V}}_{N+1}^\sigma = \mathcal{V}_{N+1}^\sigma = \mathcal{V}_0^\sigma$ is a vertex of \mathcal{K}_N . In order that $\tilde{\mathcal{V}}_{N+1}^{-\sigma} \in \Pi_{n^{-\sigma}}$, the slope of \mathcal{L}_{n^σ} must be no greater than the slope of \mathcal{L}_{N+1} (both in absolute value), and line $\mathcal{L}_{n^{-\sigma}}$ must be in the same generic conditions as before. Therefore, $|\cot(N+1)\theta| \geq |\cot n^\sigma\theta|$ and $\cos n^{-\sigma}\theta \geq 0$.

Applying the fundamental identity of trigonometry, it follows that the first inequality is equivalent to

$$\sin^2 n^\sigma\theta \geq \sin^2(N+1)\theta$$

and

$$0 \leq \sin^2 n^\sigma\theta - \sin^2(N+1)\theta = -\sin(N+n^\sigma+1)\theta \cdot \sin n^{-\sigma}\theta.$$

Since $-\sigma$ is the sign of $\sin n^{-\sigma}\theta$, we conclude that

$$\sigma \sin(2n^\sigma + n^{-\sigma})\theta \geq 0.$$

■

We just obtained a necessary condition for the strict invariance of \mathcal{K}_N . In this way, we say that the self-similar polygon \mathcal{K}_N is a *possible strictly invariant polygon* if it verifies either of the conditions in Proposition 7.

Proposition 8 *Let $\theta \in (0, \pi)$ such that $\theta \neq 2\pi/3$. The following statements hold:*

- (a) *There exists $\bar{a} > 1$ such that $\mathcal{K}_{N(\bar{a})}$ is a possible strictly $\Gamma_{\bar{a}, \theta}$ -invariant polygon.*
- (b) *If $\mathcal{K}_{N(\bar{a})}$ is a possible strictly $\Gamma_{\bar{a}, \theta}$ -invariant polygon for some $\bar{a} > 1$, then $\mathcal{K}_{N(a)}$ is a possible strictly $\Gamma_{a, \theta}$ -invariant polygon for all $a \in (1, \bar{a}]$.*

Proof We only prove statement (b). Let $[a_j, a_{j-1})$ be the interval obtained in Theorem 1 containing \bar{a} . Since n^+ and n^- remain constant on $[a_j, a_{j-1})$, then $\cos n^+\theta \geq 0$ and $\cos n^-\theta \geq 0$ for every $a \in (a_j, a_{j-1})$. Assume first that $\bar{a} > a_j$. In particular, $\mathcal{K}_{N(a)}$ is a possible strictly invariant polygon for every $a \in (a_j, \bar{a})$. On the other hand, if $a = a_j$ then

$$\sigma \sin(2n^\sigma + n^{-\sigma})\theta = \cos n^\sigma\theta |\sin(N+1)\theta| + |\sin n^\sigma\theta| \cos(N+1)\theta \geq 0$$

because $\cos n^+\theta \geq 0$ and $\cos n^-\theta \geq 0$ implies $\cos(N+1)\theta \geq 0$. So $\mathcal{K}_{N(a_j)}$ is a possible strictly invariant polygon.

By induction we only have to prove that $\mathcal{K}_{N(a)}$ is possibly strictly invariant for $a \in (a_{j+1}, a_j)$. This is straightforward since on that interval we have $n^\sigma = N_j + 1$ and $n^{-\sigma} = n_j^{-\sigma}$.

Assume now that $\bar{a} = a_j$ and $\cos n^\sigma\theta < 0$. Since $\sigma \sin(2n^\sigma + n^{-\sigma})\theta \geq 0$, then

$$|\sin n^\sigma\theta| \cos(N+1)\theta \geq -\cos n^\sigma\theta |\sin(N+1)\theta| \geq 0,$$

so $\cos(N+1)\theta \geq 0$, and therefore $\mathcal{K}_{N(a)}$ is possibly strictly invariant for $a \in (a_{j+1}, a_j)$. ■

Remark 4 For each $\theta \in (0, \pi)$, let $\bar{a} = \bar{a}(\theta)$ be the supremum of the set of values of a for which $\mathcal{K}_{N(a)}$ is a possible strictly $\Gamma_{a, \theta}$ -invariant polygon. If $\bar{a} > 1$, then $\mathcal{K}_{N(a)}$ is a possible strictly $\Gamma_{a, \theta}$ -invariant polygon for all $1 \leq a < \bar{a}$ by Proposition 8. In this case, note that \bar{a} is a bifurcation value for θ . It could be that $\mathcal{K}_{N(\bar{a})}$ is not a possible strictly invariant polygon.

Now we prove Theorem B:

Proof (Theorem B) Let

$$B_a = \{(x, y) \in \mathbb{R}^2 : y_0^- < y < y_0^+\}.$$

For all $a \in (1, \bar{a})$, since $\mathcal{K}_{N(a)}$ is a possible strictly $\Gamma_{a, \theta}$ -invariant polygon by remark 4, then both \mathcal{V}_{N+1}^\pm and $\tilde{\mathcal{V}}_{N+1}^\pm$ belong to B_a . On the other hand, the rectangle

$$C_a = \{(x, y) \in B_a : 0 \leq x \leq 1\}$$

is contained in $\mathcal{R}_{N(a)}$ by convexity. Therefore, since $x_{N+1}^\pm \rightarrow 1$ as $a \rightarrow 1$, then $\tilde{\mathcal{V}}_{N+1}^\pm \in C_a \subseteq \mathcal{R}_{N(a)}$ for all $a > 1$ sufficiently close to 1. ■

4 Existence of second-rate strictly invariant sets

In section 3, we have seen that, for all $\theta \neq 2\pi/3$, the self-similar polygons $\mathcal{K}_{N(a)}$ are (first-rate) strictly invariant for all $a > 1$ sufficiently close to 1. For larger values of a , these polygons are not necessarily strictly invariant. If they are not, then $\mathcal{K}_{N(a)}$ is strictly contained in $\Gamma_{a,\theta}(\mathcal{K}_{N(a)})$. Therefore, in this case, the consecutive images of $\mathcal{K}_{N(a)}$ under $\Gamma_{a,\theta}$ form a non-decreasing sequence of sets that converge to a second-rate strictly invariant compact set, namely the closure of $\mathcal{K} = \bigcup_{k=0}^{\infty} \Gamma_{a,\theta}^k(\mathcal{K}_N)$ (provided that it is bounded). These arguments allow to state directly the next result.

Proposition 9 *Let $(a, \theta) \in \Delta$. If \mathcal{K}_N is not strictly invariant, then \mathcal{K}_N is strictly contained in $\Gamma_{a,\theta}(\mathcal{K}_N)$. In particular, the union $\bigcup_{k=0}^{\infty} \Gamma_{a,\theta}^k(\mathcal{K}_N)$ is a second-rate strictly invariant set.*

Let us illustrate what we have said to the particular case $\theta = 2\pi/3$. In this case, the self-similar triangle $\mathcal{K}_{N(a)}$ is not even a possible strictly invariant polygon for any $a > 1$. However, we will see that there exist values of $a \in (1, \sqrt{2}]$ for which we can find second-rate strictly invariant compact sets obtained by a finite number of iterates $\bigcup_{k=0}^m \Gamma_{a,\theta}^k(\mathcal{K}_{N(a)})$ for some $m \in \mathbb{N}$.

In Figure 5 it is represented the construction of one of these second-rate strictly invariant compact sets for $a = 1.27$ from the first five iterates of $\mathcal{K}_{N(a)}$. See in Figure 7a how the attractor numerically obtained for these values of the parameters adjusts to \mathcal{K} thus showing that \mathcal{K} is a second-rate strictly invariant minimal set.

In Figure 6 it is represented the construction of one of these second-rate strictly invariant compact sets for $a = 1.19$. However, in this case, see Figure 7b, the non-simply connected attractor is strictly contained in \mathcal{K} , so that \mathcal{K} is not minimal.

Another attractor is numerically found for $a = 1.12$. In this case, as can be seen in Figure 7c, this attractor is formed by three connected components and is again strictly contained in \mathcal{K} .

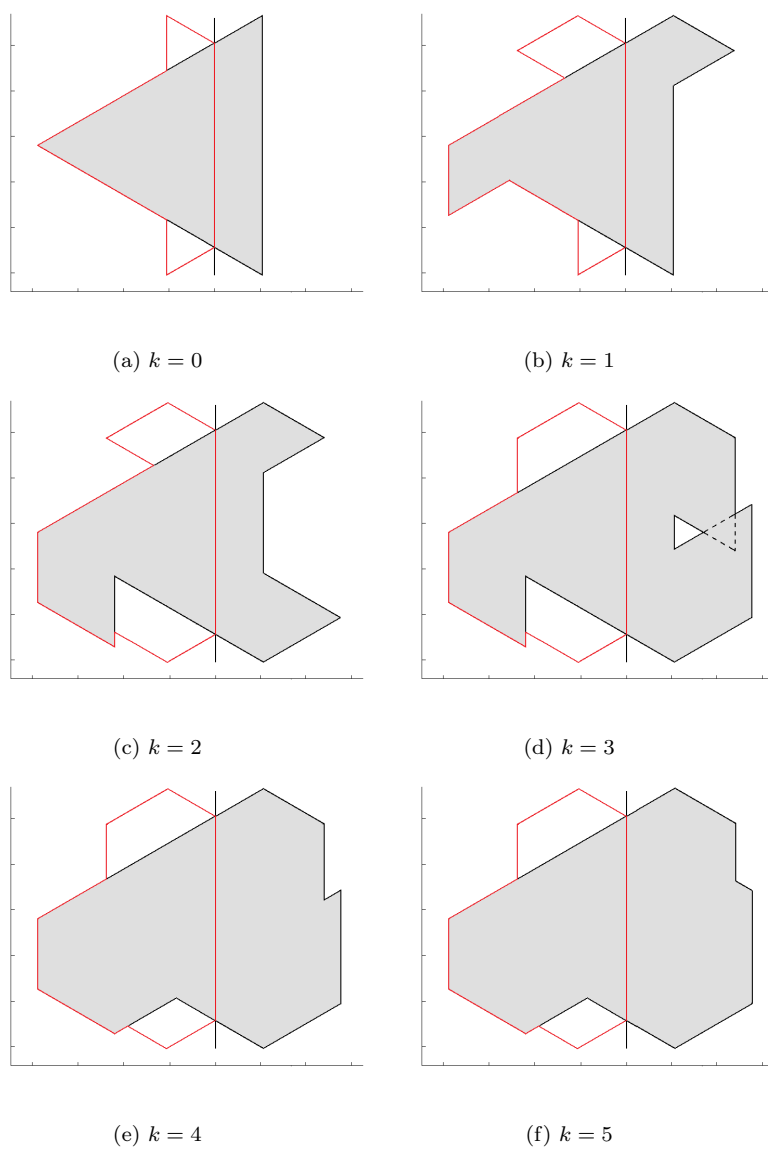


Fig. 5: Construction of the strictly invariant set $\Gamma_{a,\theta}^5(\mathcal{K}_{N(a)})$ for $a = 1.27$ and $\theta = 2\pi/3$. In grey, the k -th iterate of $\mathcal{K}_{N(a)}$ for $k = 0, 1, \dots, 5$. In red, the set $\mathcal{F}_{\mathcal{C},\mathcal{O}}(\Gamma_{a,\theta}^k(\mathcal{K}_{N(a)}))$. Note that $\mathcal{F}_{\mathcal{C},\mathcal{O}}(\Gamma_{a,\theta}^4(\mathcal{K}_{N(a)})) = \mathcal{F}_{\mathcal{C},\mathcal{O}}(\Gamma_{a,\theta}^5(\mathcal{K}_{N(a)}))$.

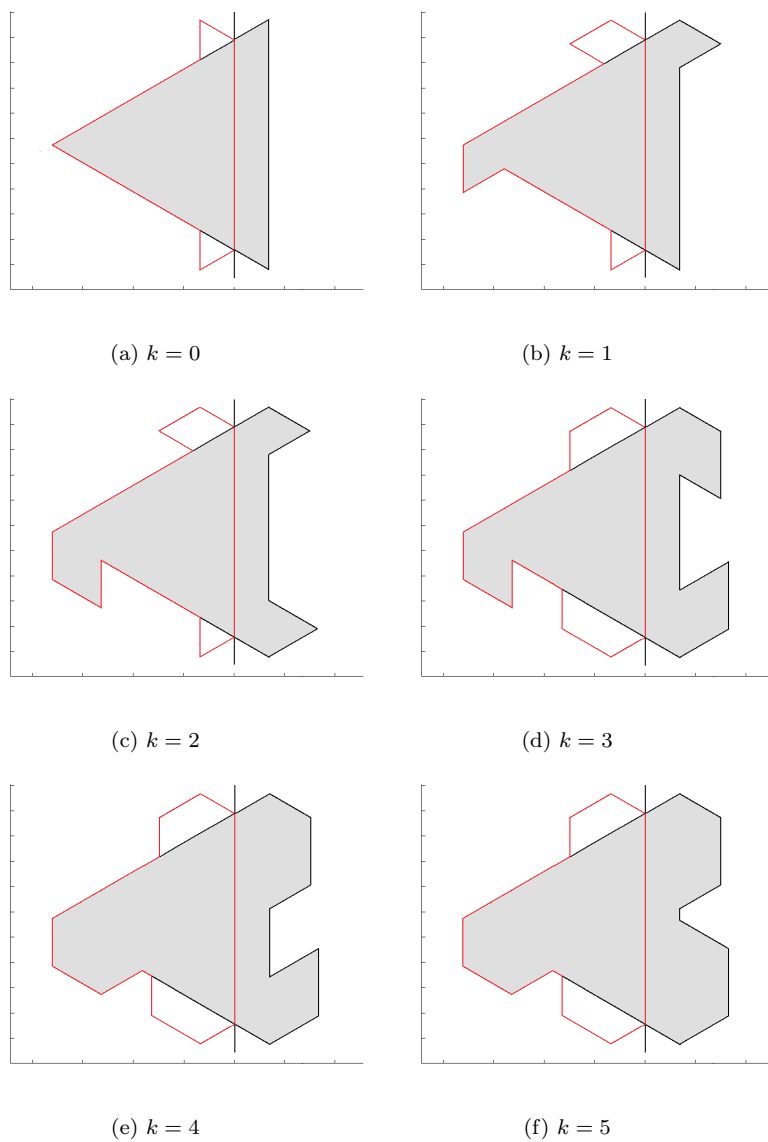


Fig. 6: Construction of the strictly invariant set $\Gamma_{a,\theta}^5(\mathcal{K}_{N(a)})$ for $a = 1.19$ and $\theta = 2\pi/3$. In grey, the k -th iterate of $\mathcal{K}_{N(a)}$ for $k = 0, 1, \dots, 5$. In red, the set $\mathcal{F}_{C,O}(\Gamma_{a,\theta}^k(\mathcal{K}_{N(a)}))$. Note that $\mathcal{F}_{C,O}(\Gamma_{a,\theta}^4(\mathcal{K}_{N(a)})) = \mathcal{F}_{C,O}(\Gamma_{a,\theta}^5(\mathcal{K}_{N(a)}))$.

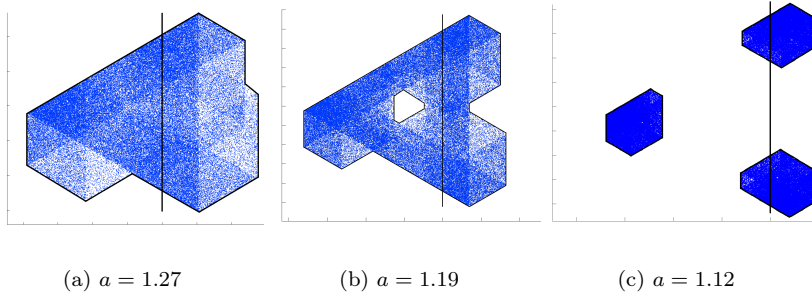


Fig. 7: Numerical attractors for $\theta = 2\pi/3$. Note that the first attractor fills the strictly invariant set, and therefore it is minimal, while the second and third one do not.

5 Attractors for 2-D tent maps: open problems

If an invariant compact polygon \mathcal{K}_N is minimal (i.e. contains no invariant compact set with non-empty interior different from itself), then it is an attractor by definition. Recall that, in this case, this polygon has to be strictly invariant. It contains a dense orbit with two positive Lyapunov exponents and, therefore, it will be a two-dimensional strange attractor.

Let $\mathcal{K}_N^* = \mathcal{K}_N \setminus \mathcal{R}_N$. Numerical experiments suggest that \mathcal{K}_N is minimal if and only if $\mathcal{O} \in \mathcal{F}_{\mathcal{C}, \mathcal{O}}(\mathcal{K}_N^*)$, that is, if and only if $(2, 0) \in \mathcal{K}_N^*$. As a decreases, the $\mathcal{F}_{\mathcal{C}, \mathcal{O}}(\mathcal{K}_N^*)$ shrinks and there comes a point that \mathcal{O} does not belong to it. Then, a new minimal strictly invariant compact set $\mathcal{A} \subsetneq \mathcal{K}_N$ turns up. At first, \mathcal{A} continues to be connected, but not simply connected: a hole around \mathcal{O} takes place. Then, \mathcal{A} splits into an increasing number of connected components as $a \rightarrow 1$. In this case, \mathcal{A} may be formed by several strange attractors and \mathcal{A} is no longer minimal. A numerical observation of this process was found in [19] for $\theta = 3\pi/4$ and is also seen in Figure 7.

An analytical proof of the results stated in the paragraph above was given in [20], [21], [22] and [23] for $\theta = \frac{3\pi}{4}$. For this value of θ , it is proved that $(2, 0) \in \mathcal{K}_N^*$ if and only if $a \geq 2^{\frac{1}{6}}$. In [20], it is proved that \mathcal{K}_N is transitive for $(1 + \sqrt{2})^{\frac{1}{4}} \leq a \leq \sqrt{2}$. In [21], for $1 < a < 2^{\frac{1}{10}}$, a certain renormalization process was introduced in order to prove the existence of a strictly invariant compact set made up of eight connected pieces. A second renormalization exists as $a \rightarrow 1$ that allows to prove the coexistence of two strictly invariant compact sets. Later, in [22], it is proved the existence of a sequence $\{a_n\} \rightarrow 1$ such that for all $a \in (1, a_n)$ the EBM $\Gamma_{a, \frac{3\pi}{4}}$ is n -times renormalizable. These renormalization procedures allowed us to prove the existence of a sequence of intervals I_n such that for each $a \in I_n$ there coexist 2^n strictly invariant compact sets for $\Gamma_{a, \frac{3\pi}{4}}$. In fact, according to Theorem 1.2 in [23], the strictly invariant compact sets obtained in [21] and [22] are strange attractors themselves or contain a certain strange attractor.

A long task is to be done beyond this work. First, proving if in all cases \mathcal{K}_N is minimal whenever $(2, 0) \in \mathcal{K}_N^*$. Second, checking if the same kind of results proved for $\theta = 3\pi/4$ can be obtained for other values of θ . Among such mentioned results, let us remark those proving the existence of absolutely continuous invariant measures which allow us to derive, see Theorem 1.2 in [23], fruitful results relating the existence of strange attractors to the presence of invariant compact sets with non-empty interior. Theorem 1.2 in [23] is strongly based on the results given in [6], [26] and [29]. Moreover, once the existence of such measures is proved for the case $\theta = 3\pi/4$, we demonstrate, see [1] and [2], that the respective density functions vary with continuity (in the L^1 -norm) with respect to the parameter a . Finally, in [1] we also derive an entropy formula for such measures as well as prove that this entropy also varies with continuity with respect to a .

One of our next objectives is, of course, to extend all of these results for any value of θ . Although it seems to be an achievable task to get all the above results for any rational value of θ/π , certain conditions used in [1], [2] and [26] may certainly fail in the case in which θ/π is not rational.

Adding to the above ingredients the fact that the polygon \mathcal{K}_N may not be strictly invariant shows that serious difficulties can be faced.

Acknowledgements

This work has been supported by the projects MINECO-15-MTM2014-56953-P and PID2020-113052GB-I00.

References

1. Alves, J.F., Pumariño, A.: Entropy formula and continuity of entropy for piecewise expanding maps. *Ann. Inst. Henri Poincaré (C) Anal. Non Linéaire* **38**(1), 91–108 (2021)
2. Alves, J.F., Pumariño, A., Vigil, E.: Statistical stability for multidimensional piecewise expanding maps. *Proc. Amer. Math. Soc.* **145**, 3057–3068 (2017)
3. Benedicks, M., Carleson, L.: On iterations of $1 - ax^2$ on $(-1, 1)$. *Ann. Math.* **122**(1), 1–25 (1985). URL <http://dx.doi.org/10.2307/1971367>
4. Benedicks, M., Carleson, L.: The dynamics of the Hénon map. *Ann. Math.* **133**(1), 73–169 (1991)
5. Brucks, K.M., Bruin, H.: Topics from One-Dimensional Dynamics, *London Mathematical Society Student Texts*, vol. 62. Cambridge University Press (2004)
6. Buzzi, J.: Absolutely continuous invariant probability measures for arbitrary expanding piecewise \mathbb{R} -analytic maps of the plane. *Ergod. Theory Dyn. Syst.* **20**(3), 697–708 (2000)
7. Colli, E.: Infinitely many coexisting strange attractors. *Ann. Inst. Henri Poincaré* **15**(5), 539–579 (1998). URL [https://doi.org/10.1016/S0294-1449\(98\)80001-2](https://doi.org/10.1016/S0294-1449(98)80001-2)
8. De Melo, W.: Renormalization in one-dimensional dynamics. *J. Differ. Equ. Appl.* **17**(8), 1185–1197 (2011). URL <https://doi.org/10.1080/10236190902998016>
9. De Melo, W., Van Strien, S.: One-Dimensional Dynamics, *Ergebnisse der Mathematik und ihrer Grenzgebiete/ A Series of Modern Surveys in Mathematics*, vol. 3. Springer-Verlag (1993)
10. Hénon, M.: A two-dimensional mapping with a strange attractor. *Commun. Math. Phys.* **50**, 69–77 (1976)

11. Lorenz, E.: Deterministic nonperiodic flow. *J. Atmos. Sci.* **20**(2), 130–141 (1963)
12. Mañé, R.: A proof of the C^1 stability conjecture. *Publications Mathématiques de l’IHÉS* **66**, 161–210 (1987)
13. Mora, L., Viana, M.: Abundance of strange attractors. *Acta Math.* **171**(1), 1–71 (1993)
14. Newhouse, S.: The abundance of wild hyperbolic sets and non-smooth stable sets for diffeomorphisms. *Publications Mathématiques de l’IHÉS* **50**, 101–151 (1979)
15. Palis, J., Yoccoz, J.C.: Homoclinic tangencies for hyperbolic sets of large Hausdorff dimension. *Acta Math.* **172**(1), 91–136 (1994). URL <https://doi.org/10.1007/BF02392792>
16. Pumariño, A., Rodríguez, J.Á.: Coexistence and persistence of strange attractors, *Lecture notes in mathematics*, vol. 1658. Springer-Verlag (1997)
17. Pumariño, A., Rodríguez, J.Á.: Coexistence and persistence of infinitely many strange attractors. *Ergod. Theory Dyn. Syst.* **21**(5), 1511–1523 (2001). URL <https://doi.org/10.1017/S0143385701001730>
18. Pumariño, A., Rodríguez, J.Á., Tatjer, J.C., Vigil, E.: Piecewise Linear Bidimensional Maps as Models of Return Maps for 3D Diffeomorphisms. In: *Progress and Challenges in Dynamical Systems, Springer Proceedings in Mathematics & Statistics*, pp. 351–366 (2013). Proceedings of the International Conference Dynamical Systems: 100 Years after Poincaré, September 2012, Gijón, Spain
19. Pumariño, A., Rodríguez, J.Á., Tatjer, J.C., Vigil, E.: Expanding baker maps as models for the dynamics emerging from 3D-homoclinic bifurcations. *Discrete Continuous Dyn. Syst. Ser. B* **19**(2), 523–541 (2014)
20. Pumariño, A., Rodríguez, J.Á., Tatjer, J.C., Vigil, E.: Chaotic dynamics for two-dimensional tent maps. *Nonlinearity* **28**(2), 407–434 (2015)
21. Pumariño, A., Rodríguez, J.Á., Vigil, E.: Renormalizable expanding baker maps: coexistence of strange attractors. *Discrete Continuous Dyn. Syst. Ser. A* **37**(3), 523–550 (2017)
22. Pumariño, A., Rodríguez, J.Á., Vigil, E.: Renormalization of two-dimensional piecewise linear maps: abundance of 2D strange attractors. *Discrete Continuous Dyn. Syst. Ser. A* **38**(2), 941–966 (2018)
23. Pumariño, A., Rodríguez, J.Á., Vigil, E.: Persistent two-dimensional strange attractors for a two-parameter family of expanding baker maps. *Discrete Continuous Dyn. Syst. Ser. B* **24**(2), 657–670 (2019)
24. Pumariño, A., Tatjer, J.C.: Dynamics near homoclinic bifurcations of three-dimensional dissipative diffeomorphisms. *Nonlinearity* **19**(12), 2833–2852 (2006)
25. Pumariño, A., Tatjer, J.C.: Attractors for return maps near homoclinic tangencies of three-dimensional dissipative diffeomorphisms. *Discrete Continuous Dyn. Syst. Ser. B* **8**(4), 971–1005 (2007). URL <https://doi.org/10.3934/dcdsb.2007.8.971>
26. Saussol, B.: Absolutely continuous invariant measures for multidimensional expanding maps. *Isr. J. Math.* **116**, 223–248 (2000)
27. Smale, S.: Differentiable dynamical systems. *Bull. Am. Math. Soc.* **73**(6), 747–817 (1967)
28. Tatjer, J.C.: Three-dimensional dissipative diffeomorphisms with homoclinic tangencies. *Ergod. Theory Dyn. Syst.* **21**(1), 249–302 (2001). URL <https://doi.org/10.1017/S0143385701001146>
29. Tsujii, M.: Absolutely continuous invariant measures for expanding piecewise linear maps. *Invent. Math.* **143**, 349–373 (2001)
30. Yorke, J.A., Alligood, K.T.: Cascades of period-doubling bifurcations: A prerequisite for horseshoes. *Bull. Am. Math. Soc.* **9**(3), 319–322 (1983)